A Molecular Dynamics Study of a Nafion Polyelectrolyte Membrane and the Aqueous Phase Structure for Proton Transport

Shengting Cui,* Junwu Liu, Myvizhi Esai Selvan, David J. Keffer, Brian J. Edwards, and William V. Steele

Department of Chemical Engineering, University of Tennessee Knoxville, Tennessee 37996-2200

Received: September 28, 2006; In Final Form: December 19, 2006

A molecular dynamics simulation study of hydrated Nafion at water contents ranging from 5 to 20 wt % was performed to examine the structure and dynamics of the hydrated polyelectrolyte system. The simulations show that the system forms segregated hydrophobic regions consisting primarily of the polymer backbone and hydrophilic regions with an inhomogeneous water distribution. We find that the water clustering strongly depends on the water content. At low water content, only isolated small water clusters are formed. As the water content increases, it becomes increasingly possible that a predominant majority of water molecules form a single cluster, suggesting that the hydrophilic regions become connected. We characterize the atomic structures formed within the system by various atomic pair correlation functions. The water structure factor shows a peak at q values corresponding to an intercluster distance about 2.5 nm and greater. With increasing water content, the distance moves to larger values, consistent with findings from scattering experiments. We find that the degree of solvation of hydronium ions by water molecules is a strong function of water content. At 5 wt %, a majority of the hydronium ions are hydrated by no more than two water molecules, prohibiting structural diffusion. As water content increases, the hydronium ions continue to become increasingly hydrated, resulting in structures capable of forming eigen ions, a necessary step in structural diffusion. Addressing the experimentally observed fact that conductivity in these membranes abruptly drops near 5 wt %, we find that both the local structure of the poorly hydrated hydronium ions and the disconnected nature of the global morphology of the water nanonetwork at low water content should contribute to poor conductivity.

I. Introduction

Proton transport through polyelectrolyte exchange membranes is an important practical issue in fuel cell design. In recent years, there has been an increased interest in understanding the fundamental processes of proton transport in these membranes.[1,2] Many experimental studies, including neutron scattering, X-ray scattering, and other methods, have been carried out in attempts to understand the transport processes from structural and dynamical perspectives.[3−25] In hydrated Nafion membranes, the morphology of the membrane consists of segregated hydrophobic (consisting of the backbone of the polymer) and hydrophilic (consisting of water and the charged side groups of the polymer) regions. However, despite the abundance of literature on the topic, there still does not exist a clear consensus on the molecular-level morphology of hydrated Nafion and its dependence on such parameters as degree of hydration. The morphology of the latter structure is closely related to the proton-transfer process.

On the basis of experimental findings, various models[7−9,26−32] have been proposed to describe the proton transport mechanism. In the cluster-network model of Gierke and Hsu,[7,8] water organizes into spherical clusters of ∼3−5 nm in diameter, which are connected by cylindrical channels ∼1 nm in diameter. In the three-dimensional model of Tovbin and Vasyatkin,[31,32] the sulfonate groups of the polymer organize into bilayers, which form pores where the water clusters reside. However, the long-range organization of the pores remains an open question. Spherical cluster formation is also assumed in the three-phase model of Yeager and Steck,[9] which consists of the fluorocarbon, the side-chain interface, and the water phases. Central among the models is the formation of water clusters.[4] Less clear is how the clusters connect and form a continuous network to accomplish the transfer of protons.

In recent years, a number of molecular simulation studies of hydrated polymer electrolyte membranes have been published;[4,33−45] however, a clear picture regarding the cluster morphology and its connectivity has not been attained. For example, Vishnyakov and Neimark[33] studied water clustering for hydrated Nafion and found that at 12.5 wt % water and a cutoff distance of 4.5 Å, the aqueous subphase consisted of disconnected clusters of about 100 molecules in size. On the basis of the observation, the authors suggested the water and ion transport is accomplished by short-lived dynamic bridges instead of the channels between clusters. In contrast, Urata et al.[42] studied the morphology of the hydrated Nafion membrane and found using the same cutoff that a continuous aqueous phase existed at 10 wt % hydration. These authors, however, did not report the distribution of the cluster size. In this study, we investigate the hydrated Nafion membrane morphology with a quantitative cluster size distribution as a function of water content.

For the bulk aqueous solution, there has been significant progress toward understanding the proton transport process through both experiment and quantum mechanical computational studies. It has been generally established that the Zundel ion and Eigen ion complexes induced by proton sharing in aqueous

* To whom correspondence should be addressed. E-mail: scui@utk.edu.

10.1021/jp066388n CCC: $37.00
Published on Web 02/09/2007

solutions significantly enhance the proton transport process[46,47] via the Grotthuss Mechanism,[48] also referred to as structural diffusion, proton shuttling, and proton hopping. These works indicate the critical importance of the local hydrogen bonding between the hydronium ions and water molecules in facilitating the transport of protons in bulk aqueous systems.

In Nafion membranes, proton hopping can still take place, but the bulk water mechanism is perturbed by a lack of a bulklike water structure. It is known that proton transport strongly depends on water content, perhaps as a result of water cluster formation and the increased probability of Zundel and Eigen ion formation.[1,2] It is thus clearly important to understand the local structure of the hydronium ion hydration and the global structure of water cluster formation in the Nafion membrane materials. For this aim, we carried out molecular dynamics simulations on systems consisting of Nafion polymer chains, hydronium ions, and water. We examine in detail the hydration of the polymers and the hydronium ions and the formation of water clusters. We discuss in this context the implication of the hydronium hydration on the possibility of the formation the Zundel and Eigen ion complexes. By examination of the cluster distribution and the dependence on the degree of hydration, we hope to shed some light on the issue of cluster networks and connectivity in polyelectrolyte membranes.

In short, while the hydrated Nafion system has been extensively studied, the contribution of this work is to provide a comprehensive analysis of the global morphology and the local structure and describe the consequences of these configurations on both the vehicular and structural diffusion of hydronium ions. The various measures that are evaluated in this manuscript include configuration snapshots, pair correlation functions, structure factors, cluster histograms, hydronium ion hydration histograms, hydronium ion hydration lifetimes, and mean square displacements.

II. Molecular Models and Method

The chemical formula for a monomer of the Nafion polyelectrolyte molecule is[49]

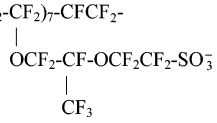

The monomer unit of the molecule consists of a backbone of CF_X groups and a side chain with two ether linkages ending in a sulfonate group. In our simulations, the polyelectrolyte molecules are composed of three monomers. Thus, each molecule has 3 side groups and 48 CF_X groups along the backbone. The backbone is terminated by CF_3 groups at the ends.

For computational efficiency, we used the united atom model for all CF_X groups in the Nafion polyelectrolyte molecules. The potential model for Nafion has been published in previous studies by other authors.[35,37,43,50−53] Consistent with the united atom model for the CF_X groups, we used the Lennard-Jones parameters developed for the CF_X groups by Cui et al.[50,51] The backbone does not carry electric charge and interacts only via Lennard-Jones and intramolecular interactions. The bond lengths, bond angles, and partial charges for the side group are given in ref 37. The force constants for bond stretching and bond angle bending are taken from Gejji et al.[52] and Cornell et al.[53] The torsional potential is from ref 43. Intramolecular sites on the same molecule separated by more than three bonds, and sites on different molecules also interact via nonbonded interactions, including the Lennard-Jones and the electrostatic (between charged sites) interactions.

The water is modeled using the TIP3P model[54,55] with a flexible OH bond.[53] The model for hydronium ions, H_3O^+, is similar to that of Urata et al.[42] In particular, the partial charges for the oxygen and hydrogen atoms are taken from Urata et al.[42] The bond distance, bond angles, and the force constants are the same as in the TIP3P model and are from refs 53−55. In the calculation of nonbonded interactions, the Lennard-Jones interaction is treated using a cutoff distance of 10 Å. The electrostatic interaction is treated with a site−site reaction field method that has been proven to be accurate.[56,57] In this method, the Coulombic interaction between charged sites is calculated within a distance of 10 Å, and the reaction field contribution is treated with a uniform background counter charge. This method has been demonstrated to be accurate for modeling aqueous ionic solutions.[56,57] We have chosen to use a relatively short Nafion polymer (3 monomers as compared to, for example, 10 monomers in Urata et al.,[42] because the fluorinated backbone of Nafion makes it a stiff polymer. As a result, it has a relatively long relaxation time compared to a hydrocarbon of the same backbone length, which increases dramatically with chain length. Because of finite computational resources, we cannot simulate for even one relaxation time of a polymer with ten monomers. Faced with this fact, one must make a choice between insufficient sampling of a longer chain and more reliable sampling of a shorter chain. Our choice to model the shorter chain is based on the approach that the model necessarily approximates reality, but the method should be reliable and reproducible. Regardless, we have thoroughly compared our results with published simulation work, such as that of Urata et al.,[42] to determine the effect of chain length, before we decided that 3 monomers was adequate.

In this study of hydrated Nafion, we included 64 polyelectrolyte molecules (192 monomers) and 192 H_3O^+, which are required to neutralize the charges. We examined the properties of the system for water contents of 5, 10, 15, and 20% of the Nafion polyelectrolyte, which correspond to the λ ratio (defined as the number of water molecules to the number of SO_3^- groups) of 3.44, 5.42, 8.63, and 11.83, respectively. This resulted in 660, 1040, 1656, and 2272 water molecules, corresponding to 7932, 9072, 10920, and 12768 total interaction sites in the simulations. The densities and water contents were chosen based on experimentally measured values.[58] For the four levels of hydration, the experimentally determined overall densities of the system are 1.95, 1.87, 1.80, and 1.74 g/cm^3. All simulations were carried out at a temperature of 300 K, and the production runs were at least 2 ns in length.

We carried out constant NVT simulations for this system. The equations of motion were integrated using the r-RESPA method[59] with a time step of 2.0 fs for the large time step and 0.4 fs for the intramolecular motions. The temperature was maintained at a constant value using the Nosé−Hoover thermostat.[60−62]

The initial configurations were created by placing molecular centers of all the molecules in the system on cubic lattice points within the simulation volume. All the atoms were initially given zero size by setting their corresponding Lennard-Jones parameters to zero. A molecular dynamics simulation was performed for 10 000 time steps in which the Lennard-Jones size parameters were gradually increased to their full values. In this way, initial configurations with non-overlapping atoms were created

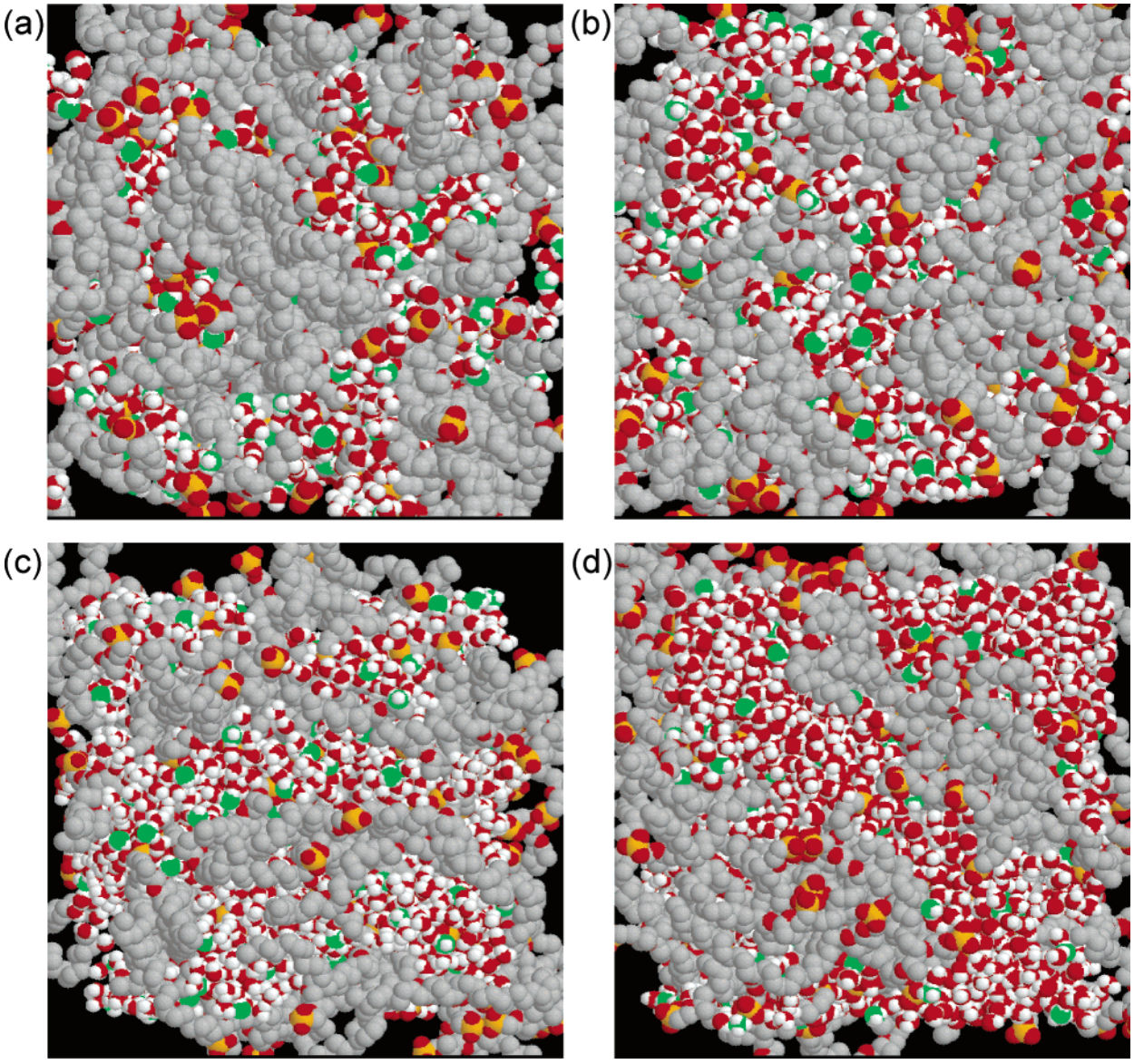

Figure 1. (a) Snapshot of the configuration at 5% water content at the end of the production run. Gray, CF_X groups; orange, sulfur; red, oxygen atom of H_2O or SO_3^-; green, oxygen atom of H_3O^+; white, hydrogen. (b) The same as (a) but at 10% water content. (c) The same as (a) but at 15% water content. (d) The same as (a) but at 20% water content.

efficiently. Equilibration using these initial configurations was then carried out for at least 2 ns before any production runs were begun.

III. Results and Discussion

In this work, we examine the structure and dynamics of hydrated Nafion. The various measures that are evaluated in this manuscript include configuration snapshots, pair correlation functions, structure factors, cluster histograms, hydronium ion hydration histograms, hydronium ion hydration lifetimes, and mean square displacements. We begin the discussion with snapshots of equilibrated configurations. In parts a−d of Figure 1, we show the snapshots of typical configurations of the hydrated Nafion for water contents of 5, 10, 15, and 20%, respectively. These snapshots generally confirm the hypothesis that the hydrated Nafion is segregated into hydrophobic and hydrophilic regions. The hydrophobic regions are constituted by the backbones of the Nafion polymer, and the hydrophilic regions are constituted by water molecules and the hydronium ions, as well as the head group of the side chains. The figures clearly show that the sulfonate groups tend to be located at the interface between the clusters and the hydrophobic regions. The hydronium ions, as displayed in green, are essentially always associated with water molecules. (See Table 1 for the average

TABLE 1: Hydration Number around Various Atomic Groups

		hydration number for different water content			
atomic types	distance	5 wt %	10 wt %	15 wt %	20 wt %
sulfur−O of H_2O	0−5.0 Å	5.47	6.87	7.68	8.19
sulfur−O of H_3O^+	0−4.8 Å	1.71	1.26	1.14	0.89
O of SO_3^-−O of H_2O	0−4.0 Å	2.38	2.96	3.23	3.42
O of SO_3^-−O of H_3O^+	0−3.5 Å	0.55	0.39	0.36	0.27
O of H_3O^+−O of H_2O	0−3.2 Å	2.25	2.76	2.97	3.15

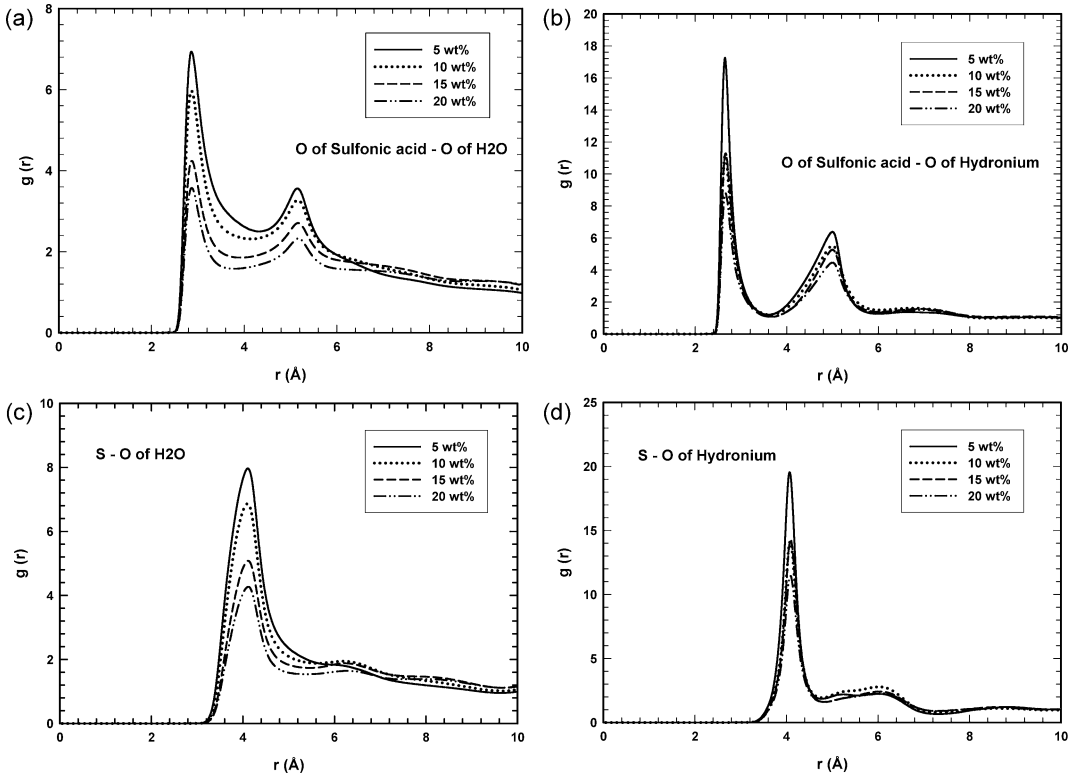

Figure 2. (a) The pair correlation function between the oxygen of the sulfonate group and the oxygen of water molecules. Solid line, 5%; dotted line, 10%; dashed line, 15%; and dash-dotted line, 20% water content, respectively. (b) The pair correlation function for oxygen of the sulfonate group and oxygen of hydronium. Line types are the same as in (a) for various water contents. (c) The pair correlation function for sulfur of sulfonate group and oxygen of water. Line types are the same as in (a) for various water contents. (d) The pair correlation function for sulfur of sulfonate group and oxygen of hydronium. Line types are the same as in (a) for various water contents.

hydration number per hydronium ion). Visual inspection suggests that at low water content, 5% by weight, the water molecules are dispersed as clusters of a few water molecules and the connectivity between the clusters is poor. As the water content increases, the cluster size increases, as does the connectivity. We defer more detailed quantitative analysis of the clusters to section III.6.

We next present various pair correlation functions (PCF) in the hydrated Nafion system. These pair correlation functions are important for several reasons. They provide information on polymer configuration (S−S correlations), on hydration of the sulfonic acid group ($S-O_{H_2O}$), on the water network ($O_{H_2O}-O_{H_2O}$), and on the hydration of hydronium ions ($O_{H_3O+}-O_{H_2O}$). This last PCF is particularly interesting since proton motion via structural diffusion is closely tied to the hydration structure of the hydronium ion.

We note that previously, Urata et al.[42] studied the sulfur−sulfur, sulfur−water, water−water, and ether oxygen−water correlation functions. In this study, we conducted a more extensive examination of the atomic pair correlation functions in order to gain insight into the structure of hydrated Nafion membranes, and in particular, we examined the sulfonate−hydronium and water−hydronium correlation functions. These additional PCFs shed some light on the structural characteristics of Zundel and Eigen ions, which are essential for proton transfer. Where possible, we have compared our PCFs with those of Urata et al.[42] in order to evaluate the effect of our shorter chains.

III.1. Pair Correlation Functions of the Sulfonate Group with Water and Hydronium. Parts a and b of Figure 2show the pair correlation functions for the oxygen atoms on the sulfonate group and the oxygen on H_2O and H_3O^+, respectively. We see two peaks at the interatomic distances of 2.9 and 5.2 Å for H_2O and 2.7 and 5.0 Å for H_3O^+, respectively. The first peak corresponds to the closest contact (the first hydration shell) between the oxygen atoms. The second peak corresponds to the second hydration shell. For the first peak, its magnitude for H_3O^+ is more than twice that of water. This can be explained by the strong electrostatic interaction between the positively charged H_3O^+ and negatively charged sulfonate oxygen. There is also a second peak between the oxygen of the sulfonate group and the oxygen of H_3O^+, corresponding to the oxygen atoms of the two groups being separated by a layer of water molecules. The existence of the second hydration peak between the sulfur and the H_3O^+ suggests that the hydronium ions are not completely bound to the sulfonate groups at all times, even though they are oppositely charged. Solvent separation of the hydronium and sulfonate ions have been previously suggested from statistical mechanical models of proton transport in Nafion.[63,64] Solvent separation has also been observed in quantum mechanical calculations of hydrated Nafion.[65] Similar solvent separated ion pair second peak was observed in previous MD work.[44] In ref 44, it is suggested that it is essential to have a reactive potential in order to describe solvent separation. In this work, we do not have a reactive potential and we observe solvent separation. We do not observe the "artificial peak" attributed to nonreactive potentials cited in ref 44. The hydronium ion can dissociate from the sulfonate group and is surrounded by water molecules.

The correlation functions between the sulfur atom of the sulfonate group and the oxygen atom of the H_2O and H_3O^+ are related to those for the oxygen of the sulfonate group and are shown in parts c and d of Figure 2. The first peaks occur at about 4 Å, and the sulfur atoms cannot be in direct contact with H_2O and H_3O^+ because of the oxygen atoms of the sulfonic acid group. In Table 1, we list the average hydration number around the sulfonate group. It shows that the average number

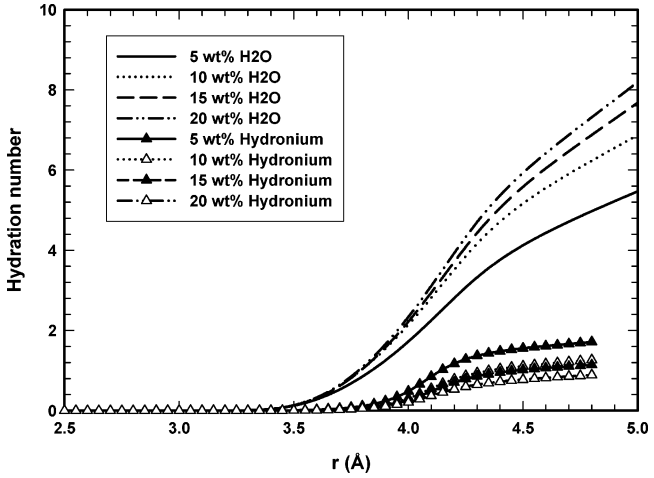

Figure 3. The number of water molecules (hydronium) around an S atom of the sulfonate. Lines, water; lines with symbols, hydronium.

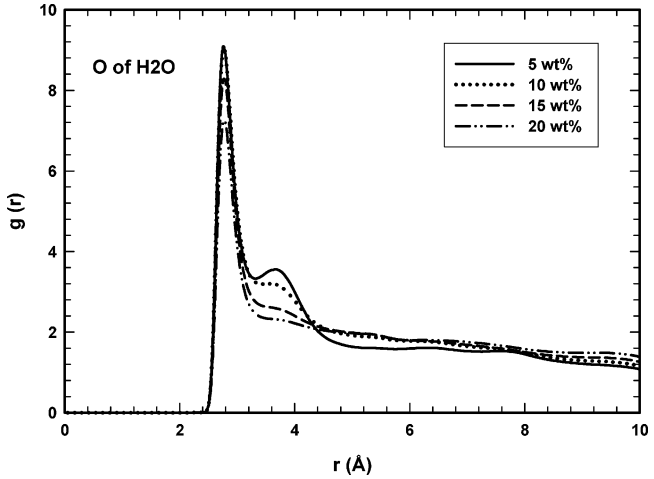

Figure 4. Water oxygen−oxygen pair correlation function.

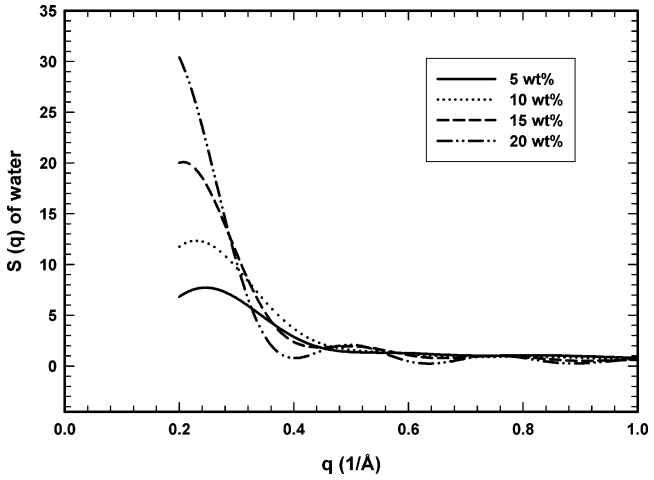

Figure 5. The structure factor $S(q)$ obtained from eq 1 for water oxygen−oxygen pair correlation function.

of H_3O^+ in the first hydration shell (contact ions) decreases with water content, while the number of water molecules increases with the water content. The increased water content increases the average number of water molecules around a sulfonate group and augments the solvation power of water and is thus more likely to pull the hydronium ion away from the sulfonate anion site. The magnitude of the peaks in Figure 2 varies from one water content value to the next. These magnitudes in part reflect a bias inherent in the pair correlation

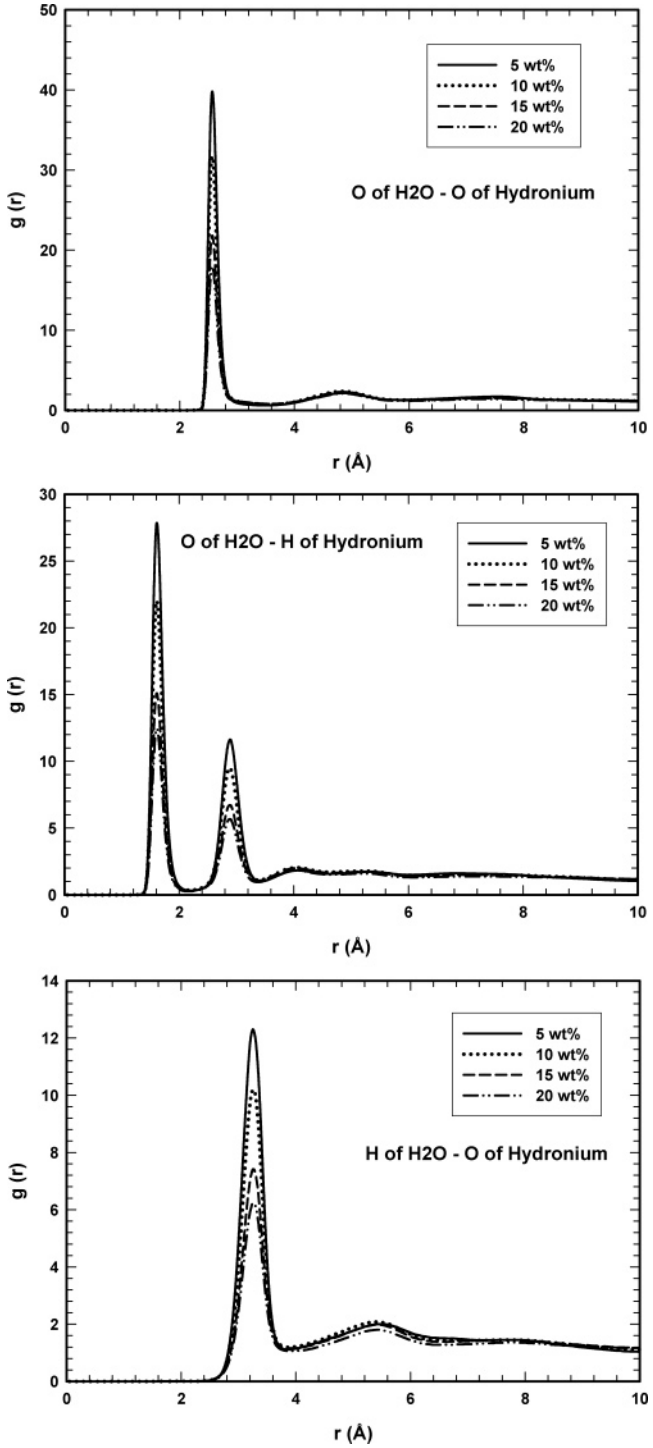

Figure 6. (a) The pair correlation function for the oxygen of water and the oxygen of hydronium. Line types are the same as in Figure 2a for various water contents. (b) The pair correlation function for the oxygen of water and the hydrogen of hydronium. Line types are the same as in Figure 2a for various water contents. (c) The pair correlation function for the hydrogen of water and the oxygen of hydronium. Line types are the same as in Figure 2a for various water contents.

function, in that, for example, the $S-O_{H_2O}$ $g(r)$ is normalized by the average water density, which changes with water content. One way to eliminate this bias is to integrate the pair correlation function up to a given distance, showing the number of molecules within that distance. The hydration shell of H_2O and H_3O^+ about the S atom is shown in Figure 3. Here we see that as one increases the water content in the system, the number of H_2O hydrating a sulfur atom steadily increases, while the number

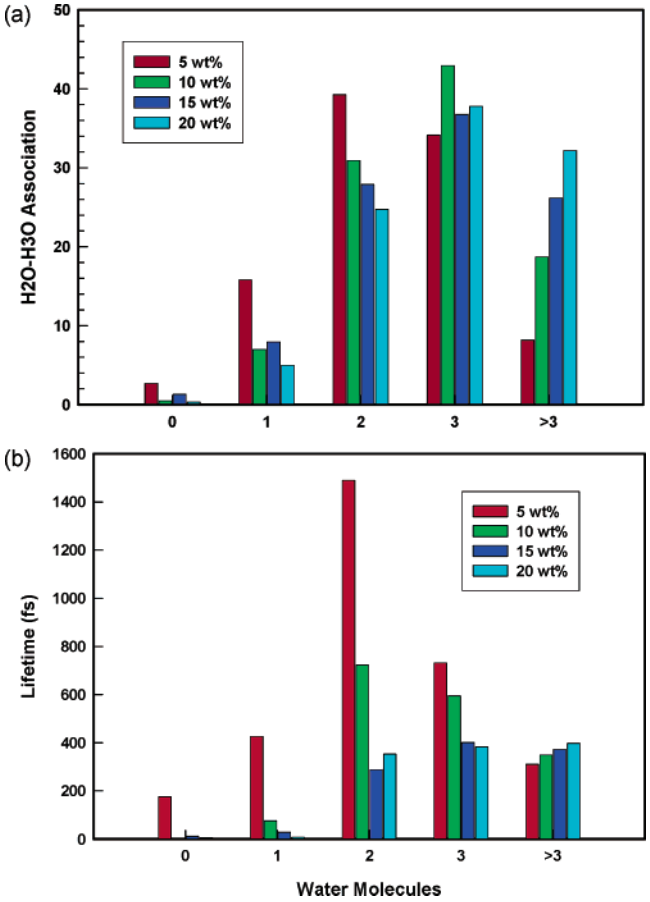

Figure 7. (a) Distribution of hydrated hydronium complexes as a function hydration number. (b) The dependence of lifetime of various hydrated hodronium complexes on the hydration number around the hydronium.

of H_3O^+ near the sulfur atom steadily decreases. Thus, the ions become more separated by the solvent, as more H_2O hydrates both the SO_3^- and the H_3O^+ ions.

III.2. H_2O-H_2O Pair Correlation Functions. Figure 4 shows the water oxygen−oxygen correlation function. The first peak occurs at 2.8 Å, corresponding to the closest contact of the two oxygen atoms. There is also a small second peak for the 5% water content, occurring at an interatomic distance of 3.7 Å. As the water content increases, the second peak becomes a shoulder and almost completely disappears. Similar behavior was also seen in the study of Urata et al.[42] The peak positions are consistent with published bulk simulation predictions for the TIP3P model.[54,55]

Many experiments have been carried out to study the characteristics of water clusters and cluster distribution. Using the calculated $g(r)$ value for water, we estimated the structure factor based on the expression

$$S(q) = 1 + \frac{4\pi N}{V}\int [g(r) - 1]\frac{\sin qr}{q} rdr \qquad (1)$$

The results are shown in Figure 5 for the water content values studied. A peak in the structure factor represents a "characteristic length scale" in the system, in this case, the "intercluster spacing" or the average distance between centers of clusters. For 5 wt % water, we observe a peak in the structure factor for 5 wt % water at a value of q corresponding to approximately 24 Å. Our data suggests that, for increasing water content, the peak shifts to lower q values. At 10 wt % water, for example, the peak occurs at a q value corresponding to a characteristic

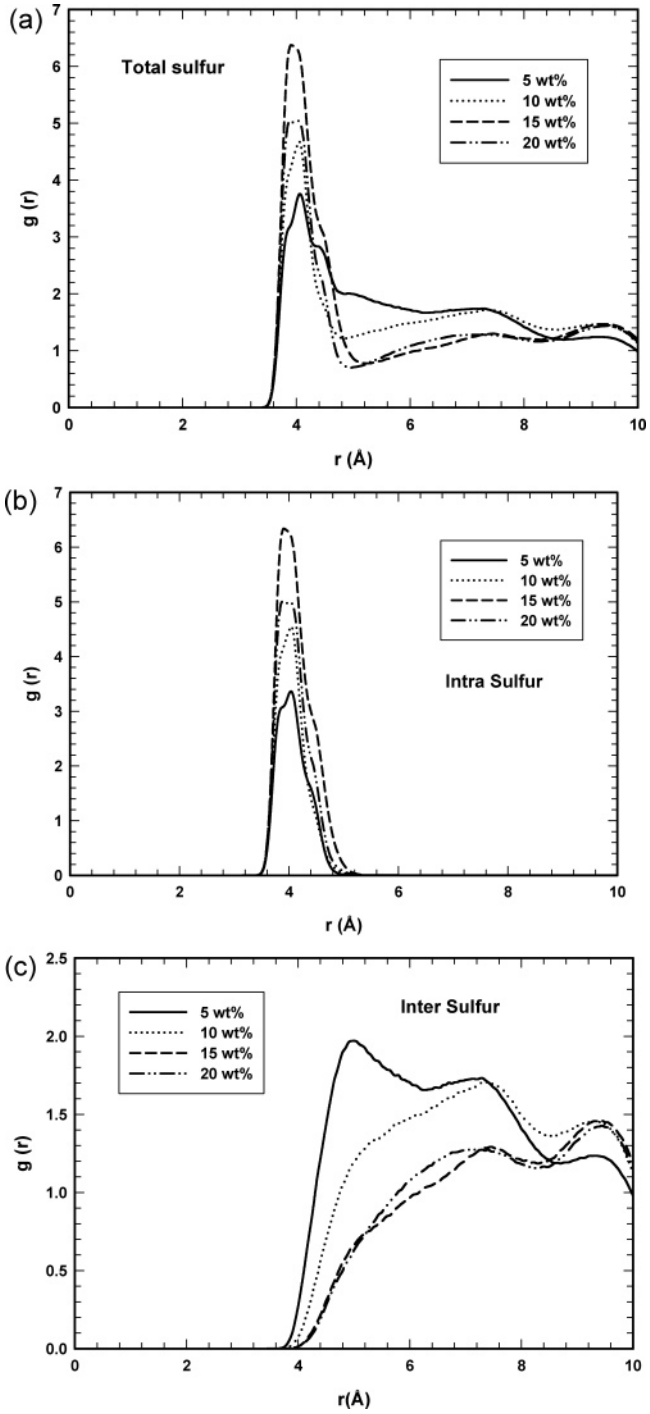

Figure 8. (a) The total sulfur−sulfur pair correlation function at various water contents. The line types are the same as in Figure 2a. (b) The intramolecular component sulfur-sulfur pair correlation function. The line types for various water contents are the same as in Figure 2a. (c) The intermolecular component sulfur−sulfur pair correlation function. The line types for various water contents are the same as in Figure 2a.

length of 26 Å, and for higher water contents the peak continues to move to smaller q (corresponding to larger intercluster distances, in agreement with established experimental findings by scattering experiments). Since our system is roughly 60 Å in each dimension, we are limited to modeling clusters up to half that size (30 Å) in this study and thus cannot say whether it is due to a complete phase segregation or a cluster of the same size.

It is important to understand that this characteristic length of twenty-odd Å does not translate into a model in which the

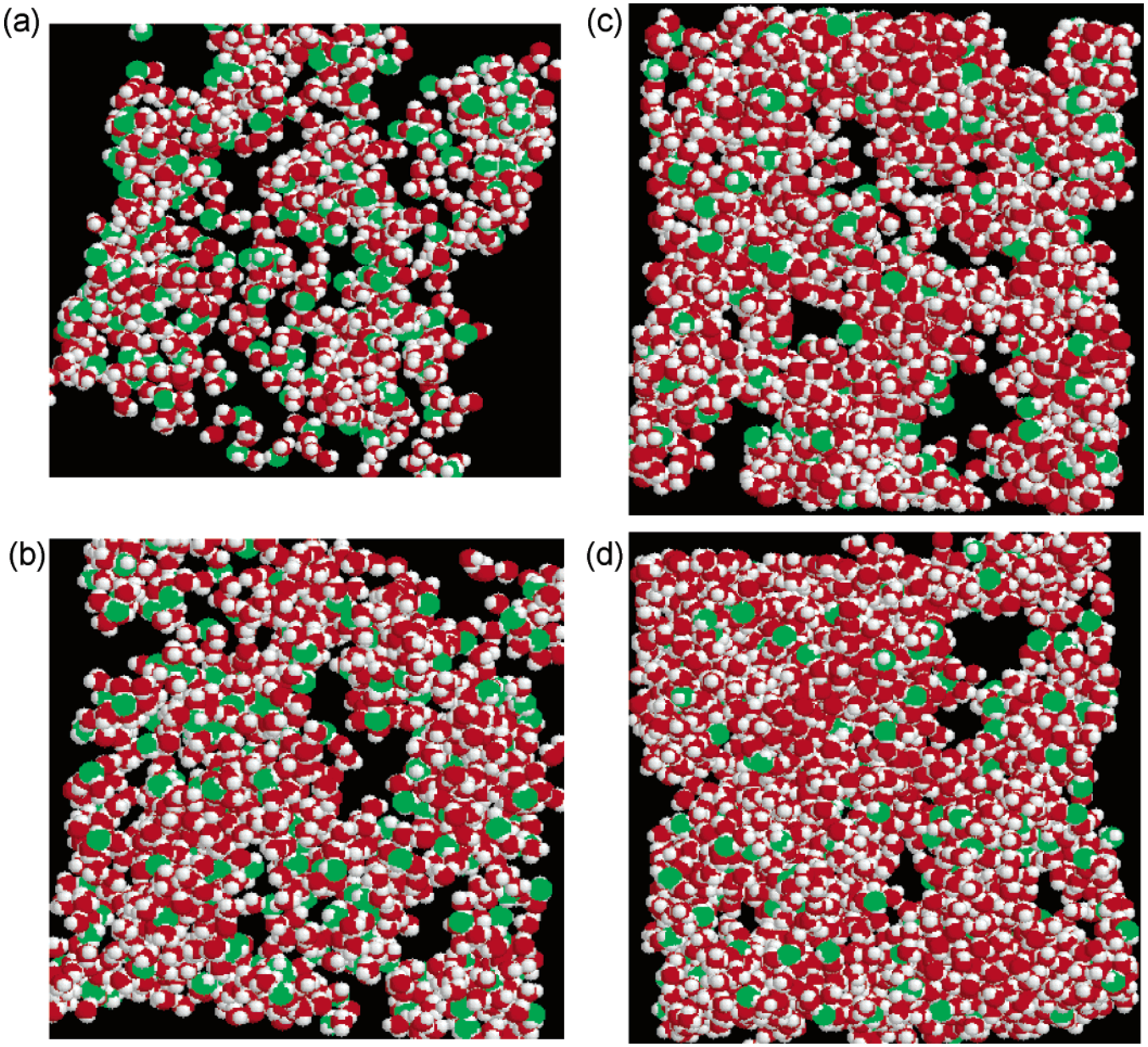

Figure 9. (a) The same configuration as in Figure 1a without showing the polymer. The color code is the same as in Figure 1a. (b) The same as in (a) but for 10% water content. (c) The same as in (a) but for 15% water content. (d) The dame as in (a) but for 20% water content.

aqueous subphase is composed of spheres of 24 or 26 Å in diameter. Rather this length scale is composed of a characteristic aqueous subphase size plus the spacing of hydrophobic phase between them. Thus the actual water clusters can be much smaller than this, as shown in parts a and b of Figure 1.

III.3. $H_2O-H_3O^+$ Pair Correlation Function. Parts a−c of Figure 6show the pair correlation functions between the H_2O and H_3O^+ at various water contents. In Figure 6a, we show the oxygen−oxygen correlation function between water and hydronium. The first peak occurs at about 2.6 Å, and the second peak occurs at a distance of 5.0 Å. There is also a slight peak at 7.6 Å. The first peak height decreases with water content, suggesting a decreased binding of water molecules to the hydronium ion caused by increased solvation effect when more water molecules are present. The solvent effect has been understood from potential of mean force theory.[57,66] Parts b and c of Figure 6 show the pair correlation function between oxygen and hydrogen of H_2O and H_3O^+; Figure 6b for water oxygen and hydronium hydrogen and Figure 6c for water hydrogen and hydronium oxygen. Although the atomic species are the same, the two pair correlation functions are clearly different. In Figure 6b, the two prominent peaks occur at distances of about 1.6 and 2.9 Å. In Figure 6c, the two peaks occur at 3.3 and 5.5 Å. The peak heights are also dramatically different. The pair correlation functions suggest that the water molecules around a hydronium ion are oriented in such a way that the oxygen atom is pointed toward the hydronium, while the hydrogen atoms are pointed away from the hydronium. This rules out the configuration where the oxygen of the hydronium forms a hydrogen bond with the hydrogen of the water molecules, which would produce a peak at 1.6 Å. This can be understood from the electrostatics: since the hydronium ion is positively charged, and the hydrogen of the water molecule carries a positive partial charge, the hydrogen atoms of the water molecules are pushed away from the hydronium.

III.4. Hydration of the Hydronium Ions. Since the hydronium ions are the counterions of the sulfonate group of the polymer, they tend to be near the sulfonate ions. At the same time, these ions can also be hydrated by highly polar water molecules. The hydration numbers for some of the atoms in

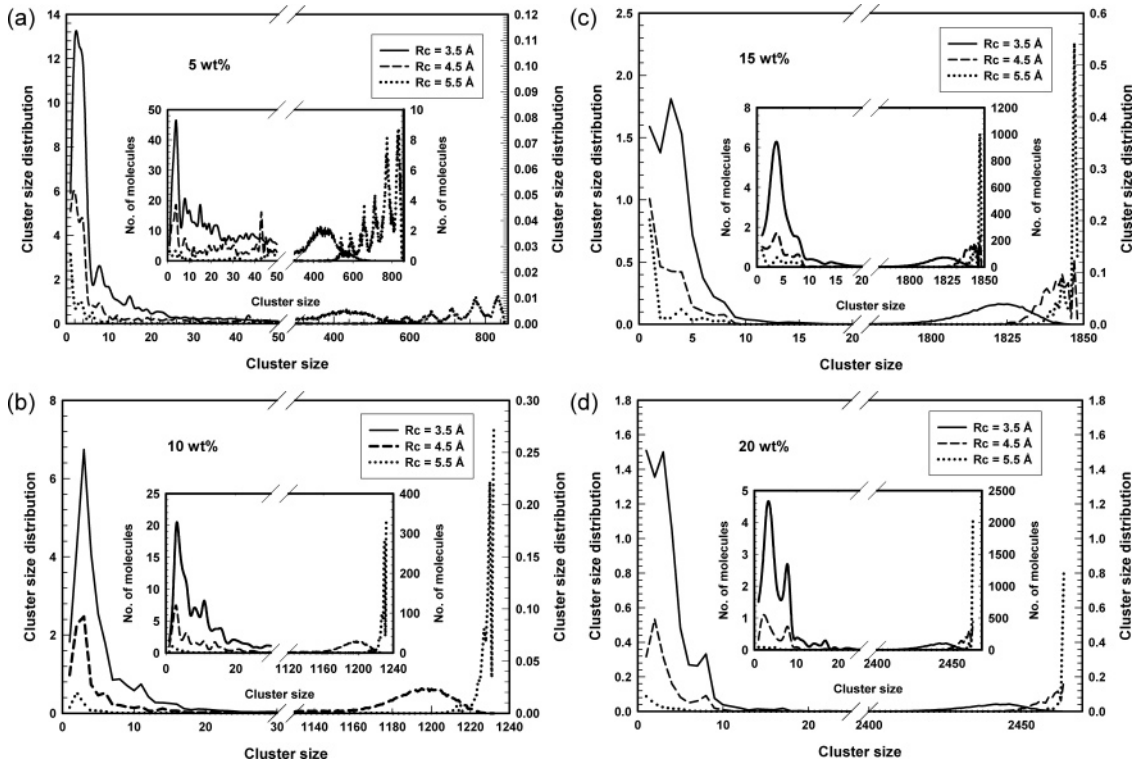

Figure 10. (a) Water cluster distribution for 5% water content averaged over 2 ns duration. Solid line, cutoff distance for molecules belonging in the same cluster is 3.5 Å; dashed line, cutoff distance is 4.5 Å; dotted line, cutoff distance is 5.5 Å. Inset: the average number of water molecules in a particular cluster size. (b) The same as (a) but for 10% water content. (c) The same at (a) but for 15% water content. (d) The same as (a) but for 20% water content.

the polymer and the hydronium are listed in Table 1. It is seen that the hydration number increases with the water content. This simply reflects the fact that there are more water molecules available as the water content increases. By comparison of the sulfonate group and the hydronium, the hydration peak of the hydronium is much higher. One reason is that the hydronium, being a free molecule, is accessible by water molecules in all directions, whereas part of the surrounding volume of sulfur is exclusive to water molecules due to intramolecular connectivity. The other is due to the tighter binding of water molecules at the shorter distance to the hydronium, which is reflected in the narrower distribution of the hydronium−water oxygen distribution (Figure 6a).

In Figure 7a, we show the probability of finding a fixed number of water molecules around a hydronium ion with a radial distance less than 3.2 Å, which includes most of the first peak in the pair correlation function. Several features are notable from this histogram. This figure clearly shows that there is a shift in the hydration distribution to higher values as the water content is increased. The probability of finding a H_3O^+ with only 1 or 2 waters within this radius strictly decreases with increasing water content. This histogram has relevance to the process of structural diffusion, which relies on the presence of an Eigen ion, requiring at least 3 waters within a 3.2 Å radius. In other words, all of the H_3O^+ with 2 or fewer waters around them are incapable of structural diffusion. In the case of 5% water, 56% of the hydronium ions have 2 or fewer waters around them. This structure can explain in part the low proton conductivity experimentally observed near 5% water. We also see that, regardless of the global morphology of the water nanonetwork, the pair correlation function can provide direct information relevant to the process of structural diffusion.

Figure 7b shows the lifetime of the hydrated hydronium complexes with none to greater than three water molecules. The monotonic decrease of the lifetime of the complex with increased hydration can be interpreted through the decreased binding energy of the water molecules to the hydronium. The hydration time is roughly in the range of picoseconds, which is sufficiently long for proton transfer to occur between the hydronium and a hydration water molecule. Experiments suggest that the lifetime of Zundel and Eigen ions is less than about 0.1 ps.[67] We do not see the strong dependence of the dynamics of hydronium hydration on water content as we did for the structure of the hydronium hydration in Figure 7a.

III.5 Sulfur−Sulfur Correlation Function. The sulfur−sulfur correlation functions are displayed in parts a−c of Figures 8. Figure 8a shows the total correlation functions, and parts b and of Figure 8 show the intramolecular and intermolecular components of the correlation function. As shown, the correlation function displays a peak at approximately 4.0 Å. From parts b and c of Figure 8, it is seen that the peak is largely due to the intramolecular sulfur−sulfur correlation. At low water content, the sulfur−sulfur intermolecular correlation function shows that the sulfur atoms have a tendency to stay closer together, probably due to the higher population of smaller water clusters, as discussed below.

The non-monotonic trend of the intramolecular component of the S−S pair correlation function is the sole qualitative discrepancy between this work and the previous work of Urata et al.[42] We attribute this difference to the fact that our chains contained 3 monomers, while those of Urata et al.[42] contained 10 monomers. In our case, we have far fewer intramolecular interactions, resulting in a larger degree of statistical uncertainty in this specific property. In these simulations, we found no other property significantly affected by chain length.

III.6. Water Cluster Distribution. For a clear visualization of the clusters and their connectivity, we show in parts a−d of

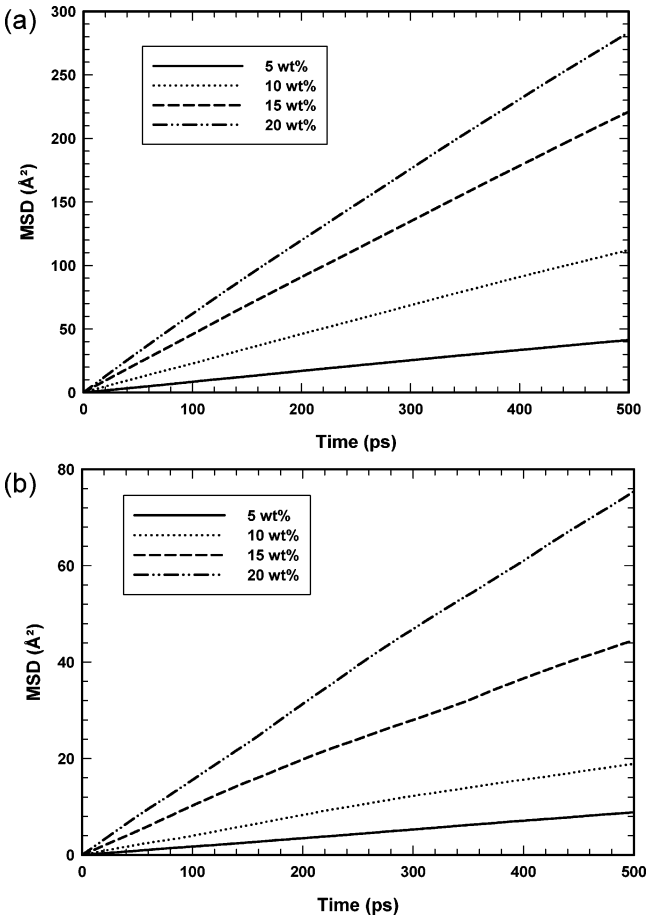

Figure 11. (a) Mean square displacement of water molecules in hydrated Nafion for water contents between 5 and 20 w t%. (b) Mean square displacement of hydronium ions in hydrated Nafion for water content between 5 and 20 wt %.

Figure 9 the snapshots of Figure 1 without the polymers. Interactive structures are available on the web,[68] where the ability to rotate the structure enables the eye to appreciate more fully the nature of the structure. In all cases, the water network is composed of many narrow, interconnecting nanochannels. For 5% water content, these figures show that the water molecules are dispersed and that there are many voids. At high water content, there are fewer voids and the water molecules in the clusters appear to be more densely packed. To characterize the clusters quantitatively, we calculated the cluster size distribution using cutoff distances of 3.5, 4.5, and 5.5 Å. Two water molecules (including the hydronium ions) are deemed to belong to the same cluster if their intermolecular distance is determined to be smaller than the cutoff distance. These are displayed in parts a−d of Figure 10. The 3.5-Å distance roughly includes all water molecules in the first hydration shell, and the 4.5 Å distance also includes the second hydration shell. In the figures, we plotted the number of clusters vs the cluster size. The inset shows the total number of molecules (including both water and hydronium) corresponding to the particular cluster size. We include the inset because the histogram itself shows large peaks at small cluster sizes. This is misleading in terms of the distribution of molecules among clusters, since small clusters contain very few molecules. The insets show the distribution on a molecular basis.

TABLE 3: Diffusion Coefficients for Water and Hydronium

water Content	water D (10^{-6} cm^2/s)	hydronium (H_3O^+) D (10^{-6} cm^2/s)
5 wt %	1.387	0.297
10 wt %	3.755	0.636
15 wt %	7.365	1.473
20 wt %	9.405	2.523

At 15 and 20% water content, we see from the insets in parts c and d of Figure 10 that, regardless of cutoff distance in the cluster definition, the vast majority of the molecules exist in a single sample-spanning cluster. The few remaining molecules are in small isolated clusters of less than 20 molecules. At 10% water content, the same is true only for the 4.5 and 5.5 Å cutoffs. For the small cutoff, most of the molecules are now in small clusters of 20 or less. At 5 wt % water content, a single large cluster only for the 5.5-Å cutoff. For the two smaller cutoffs, we see numerous small clusters.

The trend is clear. If we focus on the 4.5-Å cutoff we see a single large cluster for 10, 15, and 20% water content. However, at 5 wt % we do not. This morphology can explain in part the experimentally observed drop in proton conductivity near 5 wt % water.

By combining the information in Figures 9 and 10, we come to the following description of the morphology of the water nanonetwork in this hydrated Nafion membrane. At low water content, 5 wt %, there are many small isolated water clusters in the membrane. At higher water contents, there is generally a single large water cluster. Smaller clusters dynamically detach and coalesce with the larger cluster. By the definition of cluster used in this study, the fact that the water (and hydronium) essentially form a single cluster reflects the connectivity of water channel networks in the system. There is, however, a significant amount of inhomogeneity in terms of water density distribution. In connection with experiment, the high-density regions would contribute more to the scattering. The average distance between the high-density regions corresponds to the experimentally observed peak in the structure factor.

We should also point out that our results for the cluster distribution are qualitatively different than those of Vishnyakov and Neimark.[33] They found small clusters at 12.5 wt % using the 4.5 Å cutoff. One explanation for the difference may be that they used potassium as the cation, rather than a hydronium ion. The stronger electrostatic interaction of the potassium ion may have served to localize the water around them.

III.7. Diffusion. We calculated the diffusion coefficient of water and the hydronium ions based on the Einstein relation.

TABLE 2: Number of Water Molecules in Small and Large Clusters

	cluster size											
	<100			>100			<200			>200		
	Rc (Å)			*Rc* (Å)			*Rc* (Å)			*Rc* (Å)		
water content	3.5	4.5	5.5	3.5	4.5	5.5	3.5	4.5	5.5	3.5	4.5	5.5
5 wt %	732	331	74	120	521	778	832	439	107	20	413	745
10 wt %	261	45	4	971	1187	1228	372	51	4	860	1181	1228
15 wt %	28	8	2	1820	1840	1846	28	8	2	1820	1840	1846
20 wt %	25	5	0	2439	2459	2464	25	5	0	2439	2459	2464

The results are presented in Table 3. Since our model for hydronium ions does not include the transfer of protons between the hydronium ions and the water molecules, the diffusion coefficient for hydronium does not include the Grotthuss mechanism. Here we simply report the vehicular diffusivities. A more accurate determination of the hydronium diffusion will be addressed in a future publication. Without the structural diffusion effect, the hydronium diffusion is significantly slower than that of the water molecules, because the hydrated water molecules around the hydronium ions significantly increase the effective size of the hydronium ions. Another factor is the relatively immobile sulfonate groups, which tend to bind to the hydronium and thus slow down the diffusion of the ion. The diffusion coefficient calculated for water molecules compares very well with that measured in experiment.[69] The water diffusion coefficient is significantly smaller than in bulk water, caused by the existence of the barriers in the membrane between clusters and the constraint of the boundary at the interface between the water cluster and the polyelectrolyte. The diffusivities of both water and the hydronium ion increase with increasing degree of hydration.

IV. Conclusions

We have performed a molecular dynamics simulation study of hydrated Nafion at water contents ranging from 5 to 20 wt % to examine the structure and dynamics of the hydrated polyelectrolyte system. The simulations showed that the system forms segregated hydrophobic regions consisting primarily of the polymer backbone and hydrophilic regions with an inhomogeneous water distribution. We found that the water clustering strongly depended on the water content. At low water content, only isolated small water clusters were formed. As the water content increased, it became increasingly possible that a predominant majority of water molecules formed a single cluster, suggesting that the hydrophilic regions became connected. The morphology of the aqueous nanonetwork showed an interconnecting matrix of thin water channels. We characterized the atomic structures formed within the system by various atomic pair correlation functions. We found that the degree of solvation of hydronium ions by water molecules was a strong function of water content. At 5 wt %, a majority of the hydronium ions were hydrated by 2 or fewer water molecules, prohibiting structural diffusion. As water content increased, the hydronium ions continued to become increasingly hydrated, resulting in structures capable of forming eigen ions, a necessary step in structural diffusion. Addressing the experimentally observed fact that conductivity in these membranes abruptly drops near 5 wt %, we found that both the local structure of the poorly hydrated hydronium ion and the disconnected nature of the global morphology of the water nanonetwork at low water content can be contributing factors to poor conductivity.

Acknowledgment. The work is supported by a grant from the U.S. Department of Energy (DOE) BES under Contract No. DE-FG02-05ER15723. This research used resources of the Center for Computational Sciences at Oak Ridge National Laboratory, which is supported by the Office of Science of the DOE under Contract DE-AC05-00OR22725.

References and Notes

(1) Kreuer, K.-D.; Paddison, S. J.; Spohr, E.; Schuster, M. *Chem. Rev.* **2004**, *104*, 4637.
(2) Paddison, S. J. *Annu. Rev. Mater. Res.* **2003**, *33*, *289.*
(3) Falk, M. *Can. J. Chem.* **1980**, *58*, 1495.
(4) Eisenberg, A. *Macromol.* **1970**, *3*, 147.
(5) Duplessix, R.; Escoubes, M.; Rodmacq, B.; Volino, F.; Roche, E.; Eisenberg, A.; Pineri, M. In *Water in Polymers*; Rowland, S. P., Ed.; American Chemical Society: Washington DC, 1980.
(6) Rodmacq, B.; Coey, J. M.; Escoubes, M.; Roche, E.; Duplessix, R.; Eisenberg, A.; Pineri, M. In *Water in Polymers*; Rowland, S. P., Ed.; American Chemical Society: Washington DC, 1980.
(7) Gierke, T. D.; Munn, G. E.; Wilson, F. C. *J. Polymer Sci. B: Polym. Phys.* **1981**, *19*, 1687.
(8) Hsu, W. Y.; Gierke, T. D. *J. Membr. Sci.* **1983**, *13*, 307.
(9) Yeager, H. L.; Steck, A. *J. Electrochem. Soc.* **1981**, *128*, 1880.
(10) Verbrugge, M. W.; Hill, R. F. *J. Electrochem. Soc.* **1990**, *137*, 886.
(11) Gebel, G. *Polymer* **2000**, *41*, 5829.
(12) James, P. J.; Elliott, J. A.; McMaster, T. J.; Newton, J. M.; Elliott, A. M. S.; Hanna, S.; Miles, M. J. *J. Mater. Sci.* **2000**, *35*, 5111.
(13) James, P. J.; McMaster, T. J.; Newton, J. M.; Miles, M. J. *Polymer* **2000**, *41*, 4223.
(14) Kreuer, K. D. *J. Membrane Sci.* **2001**, *185*, 29.
(15) Haubold, H. G.; Vad, T.; Jungbluth, H.; Hiller, P. *Electrochim. Acta* **2001**, *46*, 1559.
(16) Rollet, A. L.; Gebel, G.; Simonin, J. P.; Turq, P. *J. Polymer Sci. B: Polym. Phys.* **2001**, *39*, 548.
(17) Rollet, A. L.; Diat, O.; Gebel, G. *J. Phys. Chem. B* **2002**, *106*, 3033.
(18) Young, S. K.; Trevino, S. F.; Tan, N. C. B. *J. Polymer Sci. B: Polym. Phys.* **2002**, *40*, 387.
(19) Fujimura, M.; Hashimoto, T.; Kawai, H. *Macromolecules* **1981**, *14*, 1309.
(20) Fujimura, M.; Hashimoto, T.; Kawai, H. *Macromolecules* **1982**, *15*, 136.
(21) Roche, E. J.; Pineri, M.; Duplessix, R.; Levelut, A. M. *J. Polymer Sci. B: Polym. Phys.* **1981**, *19*, 1.
(22) Heaney, M. D.; Pellegrino, J. *J. Membr. Sci.* **1989**, *47*, 143.
(23) Elliott, J. A.; Hanna, S.; Elliott, A. M. S.; Cooley, G. E. *Macromolecules* **2000**, *33*, 4161.
(24) Lehmani, A.; Durand-Vidal, S.; Turq, P. *J. Appl. Polym. Sci.* **1998**, *68*, 503.
(25) Porat, Z.; Fryer, J. R.; Huxham, M.; Rubinstein, I. *J. Phys. Chem.* **1995**, *99*, 4667.
(26) Eikerling, M.; Kornyshev, A. A.; Stimming, U. *J. Phys. Chem. B* **1997**, *101*, 10807.
(27) Datye, V. K.; Taylor, P. L.; Hopfinger, A. J. *Macromolecules* **1984**, *17*, 1704.
(28) Mauritz, K. A.; Rogers, C. E. *Macromolecules* **1985**, *18*, 483.
(29) Mauritz, K. A.; Hora, C. J.; Hopfinger, A. J. In *Ions in Polymers*; Eisenberg, A., Ed.; American Chemical Society: Washington DC, 1980.
(30) Dreyfus, B. *Macromolecules* **1985**, *18*, 284.
(31) Tovbin, Y. K. *Zh. Fiz. Khim.* **1998**, *72*, 55.
(32) Tovbin, Y. K.; Vasyatkin, N. F. *Colloid Surf. A* **1999**, *158*, 385.
(33) Vishnyakov, A.; Neimark, A. V. *J. Phys. Chem. B* **2001**, *105*, 9586.
(34) Din, X. D.; Michaelides, E. E. *AIChE J.* **1998**, *44*, 35.
(35) Elliott, J. A.; Hanna, S.; Elliott, A. M. S.; Cooley, G. E. *Phys. Chem. Chem. Phys.* **1999**, *1*, 4855.
(36) Vishnyakov, A.; Neimark, A. V. *J. Phys. Chem. B* **2000**, *104*, 4471.
(37) Vishnyakov, A.; Neimark, A. V. *J. Phys. Chem. B* **2001**, *105*, 7830.
(38) Jinnouchi, R.; Okazaki, K. *J. Electrochem. Soc.* **2003**, *150*, E66.
(39) Spohr, E.; Commer, P.; Kornyshev, A. A. *J. Phys. Chem. B* **2002**, *106*, 10560.
(40) Commer, P.; Cherstvy, A. G.; Spohr, E.; Kornyshev, A. A. *Fuel Cells* **2002**, *2*, 127.
(41) Jang, S. S.; Molinero, V.; Cagin, T.; Goddard, W. A. *J. Phys. Chem. B* **2004**, *108*, 3149.
(42) Urata, S.; Irisawa, J.; Takada, A.; Shinoda, W.; Tsuzuki, S.; Mikami, M. *J. Phys. Chem. B* **2005**, *109*, 4269.
(43) Rivin, D.; Meermeier, G.; Schneider, N. S.; Vishnyakov, A.; Neimark, A. V. *J. Phys. Chem. B* **2004**, 8900.
(44) Petersen, M. K.; Wang, F.; Blake, N. P.; Metiu, H.; Voth, G. A. *J. Phys. Chem. B* **2005**, *109*, 3727.
(45) Petersen, M. K.; Voth, G. A. *J. Phys. Chem. B* **2006**, *110*, 18594.
(46) Tuckerman, M.; Laasonen, K.; Sprik, M.; Parrinello, M. *J. Chem. Phys.* **1995**, *103*, 150.
(47) Tuckerman, M.; Laasonen, K.; Sprik, M.; Parinello, M. *J. Phys. Chem.* **1995**, *99*, 5749.
(48) Grotthuss, C. J. T. *Ann. Chim.* **1806**, *58*, 54.
(49) Nafion, DuPont, http://www1.dupont.com/NASApp/dupontglobal/corp/index.jsp.
(50) Cui, S. T.; Siepmann, J. I.; Cochran, H. D.; Cummings, P. T. *Fluid Phase Equilib.* **1998**, *146*, 51.
(51) Li, H.-C.; McCabe, C.; Cui, S. T.; Cummings, P. T.; Cochran, H. D. *Mol. Phys.* **2003**, *101*, 2157.
(52) Gejji, S. P.; Hermansson, K.; Lindgren, J. *J. Phys. Chem.* **1993**, *97*, 3712.

(53) Cornell, W. D.; Cieplak, P.; Bayly, C. I.; Gould, i. R.; Nerz, J., K. M.; Ferguson, D. M.; Spellmeyer, D. C.; Fox, T.; Caldwell, J. W.; Kollman, P. A. *J. Am. Chem. Soc.* **1995**, *117*, 5179.

(54) Jorgensen, W. L.; J. Chandrasekhar, J.; Madura, J. D.; Impey, R. W.; Klein, M. L. *J. Chem. Phys.* **1983**, *79*, 926.

(55) Price, D. J.; Brooks, C. L. *J. Chem. Phys.* **2004**, *121*, 10096.

(56) Hummer, G.; Soumpasis, D. M.; Neumann, M. *Mol. Phys.* **1992**, *77*, 769.

(57) Cui, S. T.; Harris, J. G. *Chem. Eng. Sci.* **1994**, *49*, 2749.

(58) Morris, D. R.; Sun, X. *J. Appl. Polym. Sci.* **1993**, *50*, 1445.

(59) Tuckerman, M.; Berne, B. J.; Martyna, G. J. *J. Chem. Phys.* **1992**, *97*, 1990.

(60) Nosé, S. *Mol. Phys.* **1984**, *52*, 255.

(61) Nosé, S. *J. Chem. Phys.* **1984**, *81*, 511.

(62) Hoover, W. G. *Phys. Rev. A* **1985**, *31*, 1695.

(63) Paddison, S. J.; Paul, R.; Zawodzinski, T. A. *J. Electrochem. Soc.* **2000**, *147*, 617.

(64) Paddison, S. J.; Paul, R.; Zawodzinski, T. A. *J. Chem. Phys.* **2001**, *115*, 7753.

(65) Paddison, S. J.; Elliott, J. A. *J. Phys. Chem. A* **2005**, *109*, 7583.

(66) McQuarrie, D. A. *Statistical Mechanics*; Harper & Row: New York, 1976.

(67) Woutersen, S.; Bakker, H. J. *Phys. Rev. Lett.* **2006**, *96*, 138305.

(68) Keffer, D. J.; Esai Selvan, M.; Liu, J. Nafion Structures on the Web, http://clausius.engr.utk.edu/atoms/nafion/MainPage.html.

(69) Gong, X.; Bandis, A.; Tao, A.; Meresi, G.; Wang, Y.; Inglefield, P. T.; Jones, A. A.; Wen, W. Y. *Polymer* **2001**, *42*, 6485.